Impact Welding of Aluminum onto Copper by the Gas-Gun Method[†]

Hidefumi Date* and Masaaki Naka**

Abstract

An Aluminum projectile was impact-welded onto a copper target at an impact velocity of 200 m/s or more using the gas-gun method. The microstrucutres and element distribution in the Al/Cu joint. were analyses by scanning electron microscopy, electron probe microanalyses . The Al projectile was impact-welded on a Cu target at an impact velocity from 200 to 370 m/s. The bonding strength of Al/Cu joint showed a maximum of 140 MPa at 220 m/s. The Al projectile was separated from the copper target at an impact velocity of 370 m/s or more. The formation of the θ-CuAl$_2$ phase leads to sound welding of Al onto Cu during impact welding. The crack in the brittle θ phase cause a decrease in the bonding strength of Al/Cu joints..

KEY WORDS: (Impact Welding) (Gas-Gun Method) (Aluminum) (Copper) (Interfacial Structure) (θ-CuAl$_2$)

1. Introduction

A variety of joining have been reported for bonding materials[1]. dynamic moving energy instead of conventional thermal energy is also used. The dynamic energies reported are the explosive energy due to explosive and electromagnetic energy. Since explosive welding has been investigated using the weldability window, a welding velocity of 2000 _ 3000 m/s or more is found to be needed for acceptable welding[2]. It was reported that a projectile was impact-welded to a target at an impact velocity of about 200 m/s or more using a gas-gun method in the previous work[3], with the following results obtained. The aluminum projectile was bonded to the steel target at an impact velocity of 200 m/s or more. However, a projectile of the same materials was bonded to the copper target at a velocity from 200 to 370 m/s[4]. Here, the reasons for Al/Cu bonding not being observed at a velocity of about 370 m/s or more can be clarified.

2. Experimental Procedure

The materials used were copper (99.9 mass%) of a diameter 40 mm and a thickness 5 mm and aluminum (99.5 mass%) of a diameter 11 mm and a length 20 mm. The aluminum was annealed at 623 K for 3.6 ks. The impact face of the target was polished using polishing paper after grinding, In the gas-gun apparatus showed in **Fig. 1**, an aluminum projectile collided with a copper target at the high velocity of 200 m/s or more using highly compressed nitrogen gas. Impact welding is carried out in a vacuum chamber because the air compressed between the target and the impact face of projectile prevents welding. The impact velocity of the projectile was evaluated by measuring the time to traverse a fixed distance using a laser beam system. The bombing area was observed and measured using scanning acoustic tomograph. The microstructures and element distribution in Al/Cu joints of the specimen sliced to a thickness of about 3 mm were analyzed by means of scanning electron microscope (SEM), electron probe microanalyser (EPMA).

The bonding strength of the specimen of a thickness of 3 mm described above was measured by tension tests at a tensile speed of about 10^{-3} mm/s.

---

3. Results and Discussion

3.1 Ultrasonic image

The ultrasonic image of the Al/Cu joint impact-welded at an impact velocity of 286 m/s is shown in **Fig. 2**. The black area consist of several outer discontinuous areas, the intermediate ring and the area at the center. The areas are generated due to the folding of the projectile and have a greater bonding strength than the large area at the center. The ring appears due to the scatter of the ultrasonic wave caused by the penetration of the projectile into the target and has hardly any bonding strength. The lines of A-A' and B-B' show the cutting lines for observation of the microstrucutre.

3.2 Bonding area and strength

Effect of the impact velocity on nominal fracture strength σ_n is shown in **Fig. 3**. The nominal fracture strength is the amount of fracture force divided by the black area at the center measured from the ultrasonic image. The aluminum projectile is well impact welded to the target at an impact velocity of 210 m/s or more and the maximum fracture strength is obtained at an impact velocity of 210 m/s. The fracture strength decreases with the impact velocity and the projectile is separated from the target at an impact velocity of 370 m/s or more. As reported in the previous paper on Al/Fe joint[5],

it was observed that the area of 80% or more of the bonding area of the target has been covered by the aluminum because the bonding strength is stronger than that of aluminum[5]. The area covered by aluminum is not dependent on the impact velocity. However, **Fig. 4** indicates that the ratio of the aluminum area (At) to the bonded one (An) decreased with impact velocity, in the Al/Cu joint. Accordingly, the fracture mechanism in the Al/Cu joint is different to that in the Al/Fe joint.

3.3 Microstrucutre and element

The microstrucutre of the Al/Cu joint formed at an impact velocity of 213 m/s is shown in **Fig. 5(a)**. The reacted interfacial zone is generated and a wavy interface can be observed between the zone and the copper. The microstrucuttre magnified and X-ray image analysis of the elements can be seen in **Figs. 5 b to d**. The formation of a compound layer consisting aluminum and copper is confirmed from an X-ray image analysis. The layer contains many cracks inside and some aluminum has penetrated into the cracks. **Table 1** gives a quantitative analysis of the phase formed at the aluminum and copper interface seen in Fig. 6. It is therefore concluded that the reacted interface consists of the $\theta-$CuAl$_2$ phase refereed to an alloy phase diagram of aluminum and copper.
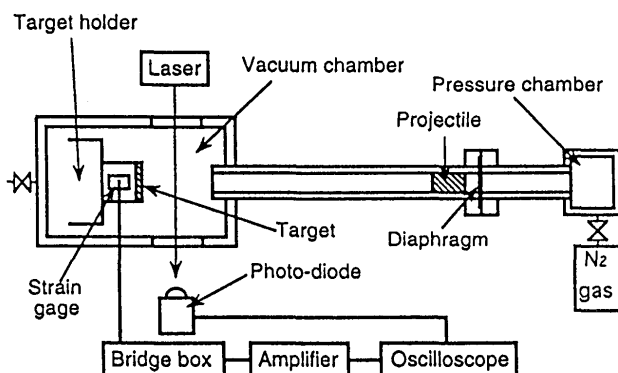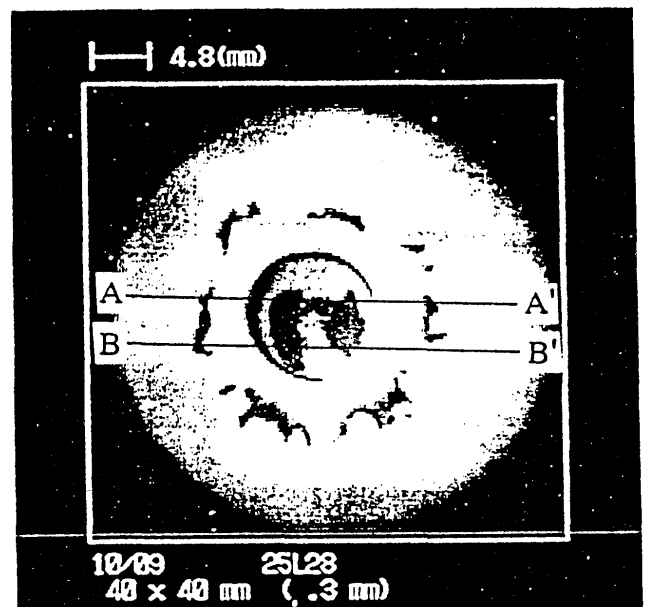

Fig. 1 Gan-gun impact welder.

Fig. 2 Ultrasonic image of Al/Cu joint welded at 333 m/s.
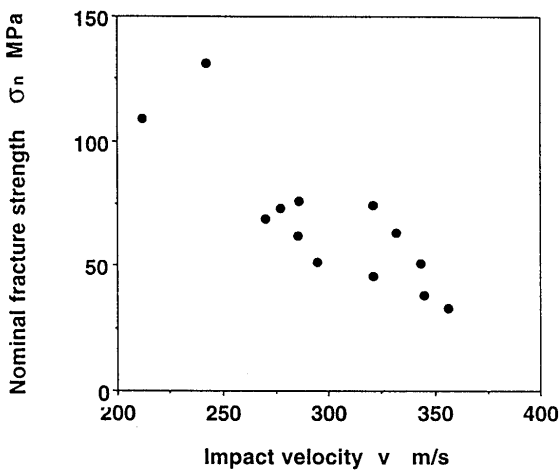
Fig. 3 Nominal fracture strength plotted against impact velocity.

Fig. 5 Microstrucuture (a,b) and X-ray image analyses of Al(c) and Cu(d) of Al/Cu joint welded at 213 m/s.
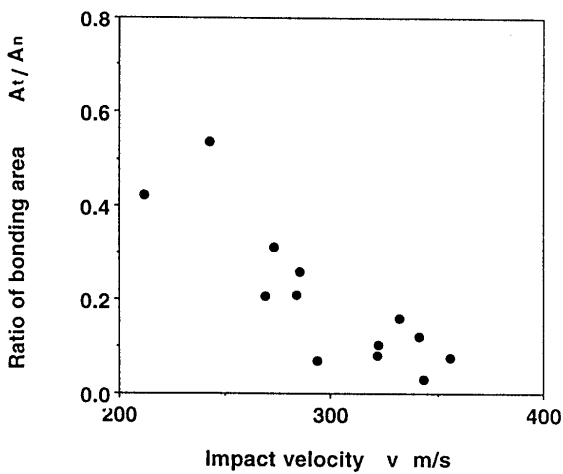

Fig. 4 Ratio of bonding area plotted against impact velocity.

Fig. 6 Microstrucuture (a,b) and X-ray image analyses of Al(c) and Cu(d) of Al/Cu joint welded at 333 m/s.
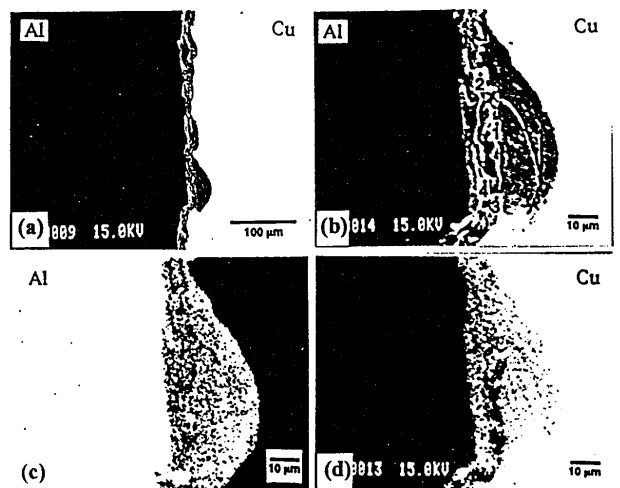
Table 1 Quantitative analyses of elements of phases formed at 213 m/s.

	Al (at%)	Cu (at%)	Si (at%)
1	74.3	25.5	0.15
2	76.0	23.8	0.16
3	97.3	1.40	1.30

Table 2 Quantitative analyses of elements of phases formed at 333 m/s.

	Al (at%)	Cu (at%)	Si (at%)
1	70.1	29.3	0.60
2	70.6	29.2	0.20
3	58.9	29.7	11.4
4	67.6	30.8	1.60

Table 3 Quantitative analyses of elements of elements on impact faces which were not welded at 213 m/s.

	Al (at%)	Cu (at%)	Si (at%)
target	61.2	38.0	0.80
projectile	83.0	15.7	1.23

The microstrucutures magnified and X-ray image analyses of the elements are shown in **Fig. 6**. The element of the interfacial microstrucutre varies as the increasing impact velocity increases. Fig. 6(a) gives the microstrucutres of the Al/Cu joint formed at the impact velocity of 333 m/s. The higher amplitude of the wavy interface than that at an impact velocity of 213 m/s is observed in Fig. 6. because the high kinetic energy is applied at the impact face and many cracks increases with the impact velocity causing the bonding strength to reduce. **Table 2** gives the quantitative analysis of the elements formed at the Al/Cu interface observed in Fig. 6. The amounts of copper and θ phase generated in the reacted interfacial zone increased because of higher kinetic energy than that at an impact velocity of 213 m/s. both impact faces of the projectile and target in which bonding was not observed at an impact velocity of 362 m/s are analyzed quantitatively using EPMA and the phases generated of 362 m/s was identified. As seen in **Table 3**, some compound of aluminum and copper could be formed in the face. Accordingly, the reason for a decrease in bonding strength with increasing impact velocity is assumed to be as follows. The compound layer was formed due to impact welding. Many cracks were generated in the compound layer due to impact velocity and caused weak bonding strength because the layer brittle and weak. Since the cracks were propagated and connected to each other in the compound at an impact velocity over about 370 m/s, impact welding due to collision of aluminum projectile with copper target could not be observed.

3.4 Estimation of temperature at impact face of projectile

It is difficult to measure exactly the temperature generated at the impact face of a projectile subjected to a longitudinal impact because a high strain gradient along the axis called mushrooming appears after impact. Accordingly the heat generation at the impact face is evaluated by a numerical analysis in this paper as follows.

Uni-axial strain is assumed to be formed at the center of an impact face of a thick projectile subjected to a longitudinal impact because no radical strain appears at the center. Since no evaluated temperature at the outer surface of the projectile is observed, the temperature at the center is higher than the others. Then, the temperature the center with uni-axial strain is estimated numerically using a strain-rate dependent equation and strain-rate independent. equation. The target is estimated to be rigid and only the temperature of the projectile is examined. An effect of conducted heat is ignored in numerical analysis.

3.4.1 Strain-rate independent constitutive equation

The following strain-rate independent constitutive equation called Hook-Reusses model (H-R model) is used[6].

$$\dot{\varepsilon} = \frac{\dot{\sigma}_{ij}}{2G} + \frac{1-2v}{E}\dot{\sigma}_m \delta_{ij} + \frac{2\sigma_{ij}}{2\overline{\sigma}H}\dot{\overline{\sigma}} \qquad (1)$$

where G is the rigidity, E is the Young's modules, δ_{ij} is the Kroneckers's delta, v is the Poison;s ration, σ_m is the mean normal stress, σ_{ij}' is the deviatoric stress, H' is the hardening coefficient, $\overline{\sigma}$ is the equivalent stress and "·" indicates differentiation by the time. The uni-axial strain model derived from Equation (1) is as follows[6].

$$\dot{\varepsilon}_1 = \frac{(1-2v)\left\{2n\overline{\sigma}(1+v) + 3E(\overline{\sigma}/\sigma^*)^{\frac{1}{n}}\right\}}{E\left\{2n\overline{\sigma}(1-v) + E(\overline{\sigma}/\sigma^*)^{\frac{1}{n}}\right\}}\dot{\sigma}_1 \qquad (2)$$

where $\overline{\sigma}$ is $\sigma_2-\sigma_1$. σ^* and n are material constants at a static stress-strain relation with n power law. The following equation gives σ_2 .

$$\dot{\sigma}_2 = \frac{2nv\overline{\sigma} + E(\overline{\sigma}/\sigma^*)^{\frac{1}{n}}}{2n\overline{\sigma}(1-v) + E(\overline{\sigma}/\sigma^*)^{\frac{1}{n}}}\dot{\sigma}_1 \qquad (3)$$

where subscripts 1 and 2 shows the loading direction and its rectangular one respectively. As all the plastic work is assumed to be converted into heat, temperature rise is obtained by the following equation.
where ρ is the density and C is the specific heat. Practically equation (2) is approximated with equation (5) except infinitesimal strain[7].

$$T = \frac{1}{\rho C}\int_0^\varepsilon \sigma_1 d\varepsilon_1 \qquad (4)$$

Then, equation (5) is substituted for equation (4). The temperature rise at a strain ε_1 is obtained by equation (6).

$$\dot{\sigma}_1 = \frac{E}{3(1-2v)}\dot{\varepsilon}_1 \qquad (5)$$

$$T = \frac{E\varepsilon_1^2}{6\rho C(1-2v)} \qquad (6)$$

3.4.2 Strain-rate dependent constitutive equation

A lot of constitutive equations in which stress depends on strain rate has been proposed so far [8]. Here, an elastic/visco-plastic body called generalized Malvern model (G-M model) is used for evaluating the temperature[9].

$$\dot{\varepsilon}_{ij} = \frac{\dot{\sigma}_{ij}}{2G} - \frac{\lambda}{2G(3\lambda+2G)}\dot{\sigma}_m \delta_{ij} + \frac{1}{2\eta}\left(1 - \frac{K}{J_2^{\frac{1}{2}}}\right)\sigma_{ij}' \qquad (7)$$

Table 4 Material and thermal constants of aluminum.

	E GPa	v	σ^* MPa	n	ρ kg/m³	C J/(kg K)
Aluminum	71	0.33	149	0.24	2688	905

where λ is the Lame' parameter, η is the coefficient of viscosity, K is the strain hardening parameter and J_2 the second variant of deviatoric stress. The following equation derived from eq. (7) shows the uni-axial strain model.

$$\dot{\varepsilon}_1 = \frac{(1+v)(1-2v)}{E(1-v)}\dot{\sigma}_1 - \frac{v}{3\eta(1-v)}\left\{\overline{\sigma} - \sigma^*\left(\int d\overline{\varepsilon}^p\right)^n\right\} \qquad (8)$$

σ_2 is obtained from the following equation.

$$\dot{\sigma}_2 = \frac{1}{1-v}\left\{v\dot{\sigma}_1 + \frac{E}{6\eta}\left[\overline{\sigma} - \sigma^*\left(\int d\overline{\varepsilon}^p\right)^n\right]\right\} \qquad (9)$$

where $d\overline{\varepsilon}^p$ is the equivalent plastic strain increment. Equation(8) and equation (9) are based on the homogeneous deformation as equations (2) and (3). Table 4 gives the material and thermal constants of aluminum used in a numerical analysis[10,11].

3.4.3 Numerical temperature

Both numerical results of the temperature rise obtained by eq. (6) and eq. (8) are shown in Fig. 7. The temperature rise-strain curves obtained by the uni-axial stress model which are the transformation of eq. (1) and eq. (7) is also given in Fig. 7 that the elevation of temperature obtained by the uni-axial strain model is about 100 times higher than that by the uni-axial stress model.

Though it is deduced that uni-axial strain occurs at the center of the impact face, the quantitative evaluation of the strain at the center is difficult. The value of the strain at the center of the impact face of projectile calculated by O'Donoghue et al. using a finite difference scheme is
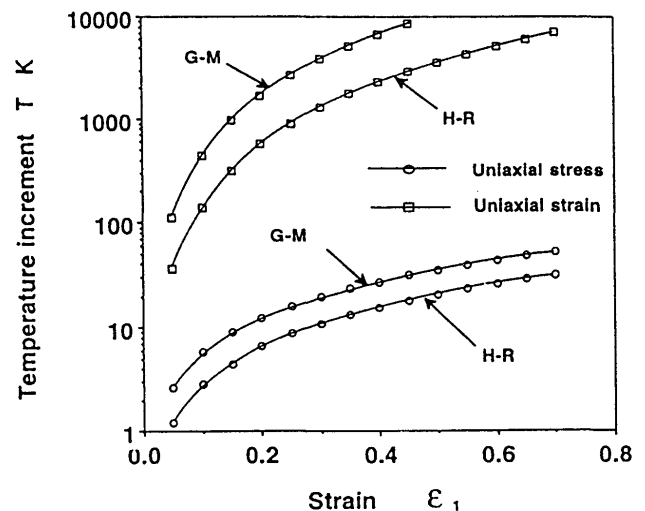

Fig. 7 Variation of numerical temperature increment against strain. G-M and H-R indicate the results obtained by strain-rate dependent and independent constitutive relations, respectively.

about 20 percent[12]. Here, the strain of 20 percent was used for the estimation of temperature at the center of impact face of a projectile. It is proved that the use of the 20 percent strain is valid by comparing both results because the stress at the center reported by them is 45 GPa and that obtained by eq. (8) is 41.5 GPa. The temperature rise generated by plastic deformation based on uni-axial strain could attain the eutectic temperature of aluminum and copper because the eutectic is 821 K, and the melting temperatures of aluminum and copper are 933 K and 1356 K, respectively. The temperature rise described above is generated only at the center of the impact face and the temperature lowers with an increasing radius. The bonding area observed in the present work and the discussion of deformation process at an impact face[13] indicate that the area of temperature rise at the impact is the 60 - 70 percent of the projectile diameter .

4. Conclusions

Aluminum was impacted onto copper by the gas-gun method, and bonding mechanism and interface microstrucutures were investigated. The following results were obtained.

The aluminum projectile was impact-welded onto a copper target at an impact velocity from 200 to 270 m/s. However, the aluminum projectile was separated from the copper target at an impact velocity of 3780 m/s or more. The formation of the θ-$CuAl_2$ phase led to sound welding of aluminum onto copper during impact welding. However, the cracks in the brittle θ phase caused a

decrease in the bonding strength of Al/Cu joints. The estimation of temperature rise at impact face suggests that the temperature rise of 1000 K or higher is generated on the neighborhood of the center of the impact face of a projectile.

References

1) H.Cary,Joinning Process, Welding, Brazing and Soldering in ASM Handbook,6.(1993), 175.
2) V. M. Ogolikhin and V.A.Simon,"Using Explosive Welding to Fabricate Blanking Dies and Punches", Metallurgical Applications of Shock-Wave and High Strain-Rate Phenomena, edited by L.E.Murr ,K.P. Staudhammer and M.A.Meyer, (1986), 917.
3) H. Date,Y.Sato,T.Abe and M.Naka, ,J.High Temp. Soc.,19,(1993),69.
4) H. Date and M.Naka, J.High Temp. Soc., 21(1995), 312.
5) H. Date and T.Abe ,J.Soc.Mat.Sci. Japan , 42 1993), 1432.
6) H. Sato, W. Takayam and Y. Shono, J. Plastic Deformation, 32(1991), 597.
7) N. Nakagawa, Impact Engineering, ed. by T. Hayashi and Y. Tanaka, Nikkannkogyo Shonbun., p45.
8) K. kishida, N. Nakagawa and K. Yokoyama, J. Plastic Deformation, K. kishida, n. Nakagawa and K. Yokoyama, J. Plastic Deformation, 17(1976), 61.
9) Data of Heat Conduction, 3rd Ed. ed by Japan Mech. Eng., 1976, p314.
10) H. Date, J. Soc. Mat. Sci. Japan, 42(1993), 517.
11) P. E. O. Donoghe, S. R. Bonder, C. E. Anderson and M. Ravid, Inst. J. Impact Eng., 8(1989), 289.
12) H. Date, J. Soc. Mat. Sci. Japan, 41(1992), 600.